ARMY RESEARCH LABORATORY

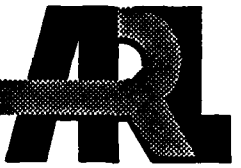

Laser Ignition of Solid Propellants: I. Ignition Delays

Arthur Cohen
Richard A. Beyer

ARL-TR-162 July 1993

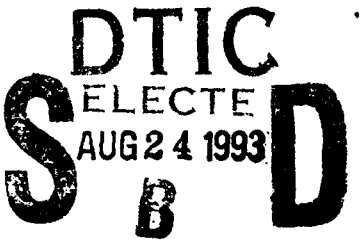

NOTICES

Destroy this report when it is no longer needed. DO NOT return it to the originator.

Additional copies of this report may be obtained from the National Technical Information Service, U.S. Department of Commerce, 5285 Port Royal Road, Springfield, VA 22161.

The findings of this report are not to be construed as an official Department of the Army position, unless so designated by other authorized documents.

The use of trade names or manufacturers' names in this report does not constitute indorsement of any commercial product.

REPORT DOCUMENTATION PAGE

Form Approved
OMB No. 0704-0188

1. AGENCY USE ONLY (Leave blank)	2. REPORT DATE	3. REPORT TYPE AND DATES COVERED
	July 1993	Final, Jan 90 - Dec 91

4. TITLE AND SUBTITLE
Laser Ignition of Solid Propellants: I. Ignition Delays

5. FUNDING NUMBERS
PR: 1L162618AH80

6. AUTHOR(S)
Arthur Cohen and Richard A. Beyer

7. PERFORMING ORGANIZATION NAME(S) AND ADDRESS(ES)
U.S. Army Research Laboratory
ATTN: AMSRL-WT-PC
Aberdeen Proving Ground, MD 21005-5066

8. PERFORMING ORGANIZATION REPORT NUMBER

9. SPONSORING / MONITORING AGENCY NAME(S) AND ADDRESS(ES)
U.S. Army Research Laboratory
ATTN: AMSRL-OP-CI-B (Tech Lib)
Aberdeen Proving Ground, MD 21005-5066

10. SPONSORING / MONITORING AGENCY REPORT NUMBER
ARL-TR-162

11. SUPPLEMENTARY NOTES

12a. DISTRIBUTION / AVAILABILITY STATEMENT
Approved for public release; distribution is unlimited.

12b. DISTRIBUTION CODE

13. ABSTRACT (Maximum 200 words)

Ignition experiments on nitrate-ester and nitramine propellants have been conducted in a closed bomb. The ignition source was a variable (<100 W) cw CO_2 laser. Ambient conditions were room temperature and atmospheric pressure. Air, argon, and nitrogen gases were used. Times to detect emission and changes in emission rate which are attributed to onset of flamespreading have been compared with ignition delay calculations using a condensed phase radiant ignition model. Reasonable values for thermochemical properties and experimental determined values for chemical kinetic parameters and optical properties were used for the calculations. The flux dependence of the initial emission delays were in reasonable agreement with model predictions for nitrate-esters but not for nitramines. Gas phase (composition) effects on initial emission were observed with XM39, an RDX nitramine, but not with nitrate-esters. Flamespreading delays showed gas composition effects with all propellants. These results suggest that (for all propellants) the effects of gas phase reactions on flamespreading and (for nitramines) on initiation need to be included (explicitly) in radiant ignition models for predicting pressurization in gun chambers.

14. SUBJECT TERMS
lasers, solid propellants, laser ignition

15. NUMBER OF PAGES
31

16. PRICE CODE

17. SECURITY CLASSIFICATION OF REPORT	18. SECURITY CLASSIFICATION OF THIS PAGE	19. SECURITY CLASSIFICATION OF ABSTRACT	20. LIMITATION OF ABSTRACT
UNCLASSIFIED	UNCLASSIFIED	UNCLASSIFIED	UL

INTENTIONALLY LEFT BLANK.

TABLE OF CONTENTS

INTENTIONALLY LEFT BLANK.

LIST OF FIGURES

INTENTIONALLY LEFT BLANK.

1. INTRODUCTION

One of the objectives of the LIGHT program is to determine the feasibility of replacing gun igniter systems with lasers. This is expected to increase safety and survivability and to improve the performance of gun systems. Models of the laser-solid propellant ignition process which can be used to calculate the initial gun chamber pressurization will help achieve this objective. By comparing model calculations with results from closed bomb experiments, the ability of (thermal) radiative ignition models to predict the response of solid propellants to laser irradiation can be evaluated.

Many radiative ignition models are available for evaluation (Kulkarni, Kumar, and Kuo 1982; Hermance 1984). They are usually classified according to the phase(s) in which the self-accelerating exothermic reaction(s) associated with the ignition process occurs (i.e., condensed, gas, heterogeneous). Most models are one dimensional and have ignition criteria based on transient temperature behavior. The physical and chemical processes which describe the "ignition" mechanism differ even in models of the same class (Kulkarni, Kumar, and Kuo 1982). To compare predictions with experimental data usually requires numerical solutions of the equations used to describe the details of these processes. Analytic solutions are possible through use of simplifying assumptions (Williams 1966). Phenomonological ignition models do not attempt detailed descriptions of the ignition processes, and the corresponding equations, in some cases (Vilyunov and Zarko 1989; Anderson 1972), have analytic solutions.

It is generally difficult to evaluate radiative ignition models due in part to difficulties of matching the experimental and model boundary conditions and relating diagnostics and model ignition criteria. In addition, the physical/optical properties and heat release rates which are required as inputs to the model are not well known. Laser ignition models may have an additional problem (i.e., describing the details of the laser energy [thermal and nonthermal] interactions with the propellant and with reaction products).

The initial results of an investigation of laser ignition of some nitrate ester (M9, M30, JA2) and nitramine composite (XM39, HMX2) solid propellants under ambient conditions will be presented, and correlations of emission and flamespreading delay measurements with predictions of a phenomonological radiant ignition model will be discussed.

2. IGNITION MODEL

The model (referred to as "approximate") is described in Vilyunov and Zarko (1989). It considers condensed phase (surface) reactions and in-depth energy absorption but neglects energy losses (i.e., those losses due to surface [film] heat transfer and emission), propellant consumption, and does not consider the effect of laser interruption (deradiation). The model is one dimensional (semi-infinite solid). It assumes that flux is continuous and uniform and that energy production can be described by a first-order (global) surface reaction. The relevant energy equation and boundary conditions used for (transparent) solids are:

$$c\frac{\partial T}{\partial t} = \alpha c\frac{\partial^2 T}{\partial x^2} - \frac{1}{\rho}\frac{\partial q}{\partial x} + Qz\exp(-E/RT)$$

$$T(x,0) = T_o;\ \frac{\partial T}{\partial x}(0,t) = 0;\ T(\infty,t) = T_o,$$

where $q = q_o\exp(-nx)$, q_o = transmitted surface flux, n = absorption coefficient, T = temperature, t = time, x = distance from irradiated surface, T_o = ambient temperature, α = thermal diffusivity, ρ = density, and c = specific heat. The last term in the energy equation is the Arrhenius global heat release rate during ignition (E = activation energy, z = first-order pre-exponential factor, and Q = heat of reaction).

The ignition delay (t_{ig}) is the sum of (inert) "heat up" (t_h) and (chemical) induction (t_{ch}) times. The surface temperature (T_h) and t_h are determined by finding the temperature at which the time derivatives obtained from analytic solution of the energy equations corresponding to inert (radiant) heating (Q = 0) and to adiabatic (spatially independent) reaction ($\alpha = q_o = 0$) become equal. T_h represents the chemical reaction temperature at which the (specific) rate of chemical energy production equals the radiant energy absorption (at the surface). t_h is the time required to reach this temperature. At later times, due to the Ahrrenius exponential temperature dependence, chemical rates dominate and it is assumed that surface reaction occurs under adiabatic conditions. The chemical induction time is obtained from the adiabatic solution and is defined (in this model) as the time (with respect to t_h) for time derivative to become infinite. Approximations to these analytic solutions (given in Vilyunov and Zarko 1989) were used to calculate T_h and the corresponding t_h and t_{ig} as a function of radiant flux. The inert approximation (for T_s and t_h) is valid under conditions when characteristic lengths for heat conduction during heat up are much greater than those for absorption ($n\sqrt{\alpha t_h} >> 1$). The adiabatic approximation (for t_{ch}) is valid

when activation energies are much greater than thermal energies ($E/RT_h >> 1$). For convenience, the derivation (along with the energy equations and their solutions) of these approximations is shown in the Appendix. In all calculations, T_o = 298 K, and for all propellants, the following values were used for the thermophysical properties: α = 0.001 cm^2/s, c = 0.35 cal/g-K, and ρ = 1.6 g/cm^3. A distinguishing feature of the model is the prediction of a (chemical kinetic-dependent) flux level above which $t_{ch} << t_h$, (i.e., $t_h = t_{ig}$). This "approximate" theory has been previously used to predict the dependence of "ignition" delays for secondary explosives (HMX, RDX) on laser flux (Vilyunov and Zarko 1989). Reasonable success was obtained using experimentally determined values for the input parameters.

3. EXPERIMENTAL

A cw CO_2 (10.6 μm) laser (Synrad model No. 51) with variable power (nominal power = 10–100 W) was used as the ignition source. Power was measured with a thermopile (Coherent Radiation model 201). The estimated measurement error is ±10%. The responses of several propellants at different power (flux) levels and in different gaseous environments have been briefly examined. Data have been obtained for the following propellants: M9 (homogeneous NC double base), JA2 (homogeneous NC triple base), M30 (composite NC triple base), XM39 (RDX composite), and HMX2 (experimental HMX composite). The samples were small cylinders approximately 3/16 in long and 0.25 in diameter. The M30 and XM39 samples were cut from grains (perforated with graphite surfaces), and the others were cut from solid strands. The beam (diameter about 3 mm) was directed horizontally along the propellant axis and covered approximately 25% of the sample (plane) surface. Pulse lengths were varied from 0.1–15 s. Delays to emission and flamespreading, denoted by t_e and t_f, were measured from emission traces recorded by a photomultiplier (300–800 nm response), which viewed the region near the irradiated surface. t_e represents the time (from start of irradiation) to detect emission, and t_f, which is a more subjective measurement, represents the time to observe a change in the slope of the emission signal consistent with onset of a relatively steady state process. This change is assumed to indicate the start of the flamespreading process. Estimated measurement errors for t_e and t_f are ±5% and 15%, respectively. Most measurements were made in a closed bomb (inside dimensions 3 in diameter by 9 in tall). The location and sensitivity of the photomultiplier were not changed for these experiments. The bomb has optical access from four sides, with one containing a ZnSe window for transmitting the 10.6-μm radiation. The bomb was initially filled with air, nitrogen, or argon. Ambient conditions were room temperature and atmospheric pressure.

An infrared (IR) microscope-spectrometer (Spectra-Tech Plan 40/Matson Polaris) was used to measure propellant reflectivities and transmittivities at 10.6 μm. Propellant reaction products were analyzed by gas chromatography and FTIR spectrometry.

4. EXPERIMENTAL RESULTS

4.1 Optical Properties. Bouguer's law was used to derive the absorption coefficients from the dependence of transmittivity on propellant width. This implicitly assumes scattering coefficients << absorption coefficients. At present, the absorption coefficients for M9, JA2, and XM39 have been determined and are 536, 250, and 756 cm^{-1}, respectively. In the visible region, the transparency of JA2 is much greater than M30 and HMX2. If this is also true at 10.6 μm, then the value of n = 250 cm^{-1}, which has been used for the absorption coefficient of M30 and HMX2 in calculations, will represent a lower bound. This leads to an upper bound for the calculated ignition delays.

The results of the initial reflectivity measurements indicate that at 10.6 μm all propellants reflect less than 10%. For comparison with calculations the measured flux values were corrected using a reflectivity value of 0.08.

4.2 Gas Product Analysis. At present, only a cursory examination of the results from gas analyses has been made. The major difference between samples from flamespreading and non-flamespreading experiments, besides concentration levels, appears to be the higher CO/CO_2 ratio for the latter.

4.3 Laser Ignition. The following figures contain photomultiplier records selected to show some of the complexities occurring during laser ignition experiments, and graphs which compare the emission and "flamespreading" delays obtained from such records with predictions of the "approximate" ignition model. For some experiments, "flamespreading" delays (t_f) were greater than the laser pulse duration (t_l). In such cases, t_l, which is a minimum lower bound for t_f, was used for the comparisons. In some cases, data represent average values of several measurements.

Listed in Table 1 are the laser power (P), t_l, and the corresponding delays (t_e, t_f, t_d) obtained from the photomultiplier signals shown in Figures 1, 3, 5, and 7. t_d is an estimate of the final emission decay time.

4.3.1 Nitrocellulose Propellants. Figure 1 shows the effect of flux levels on emission during ignition and flamespreading of M9 in nitrogen at ambient conditions. Time is relative to start of the laser irradiation. The points e, f, and d locate the emission delay, t_e; "flamespreading" delay, t_f (corresponding to a slope change in the emission-time signal); and final emission decay time, t_d. Both t_e and t_f (conceivably related to t_h and t_{ig}, respectively) decrease as power increases. The M9 emission decay at d1 and d2 is due primarily to consumption of propellant.

Table 1. Laser Operating Conditions and Delay Measurements for Figures 1, 3, 5, and 7

Figure	Signal	Laser Power (W)	t_l (s)	t_e (s)	t_f (s)	t_d (s)
1	1	2.5	5.80	0.19	0.30	1.65
	2	8.6	1.10	0.03	0.09	1.40
4	1	1.7	4.34	1.93	4.85	4.30
	2	8.6	1.67	0.05	(0.12)	1.70
6	—	4.2	2.72	0.04	1.37	3.60
8	1	8.6	0.62	0.18	2.10	0.65
	2	8.6	0.20	0.11	—	0.22

t_l = laser pulse duration
t_e = emission delay
t_f = flamespreading delays
t_d = estimate of final emission decay time

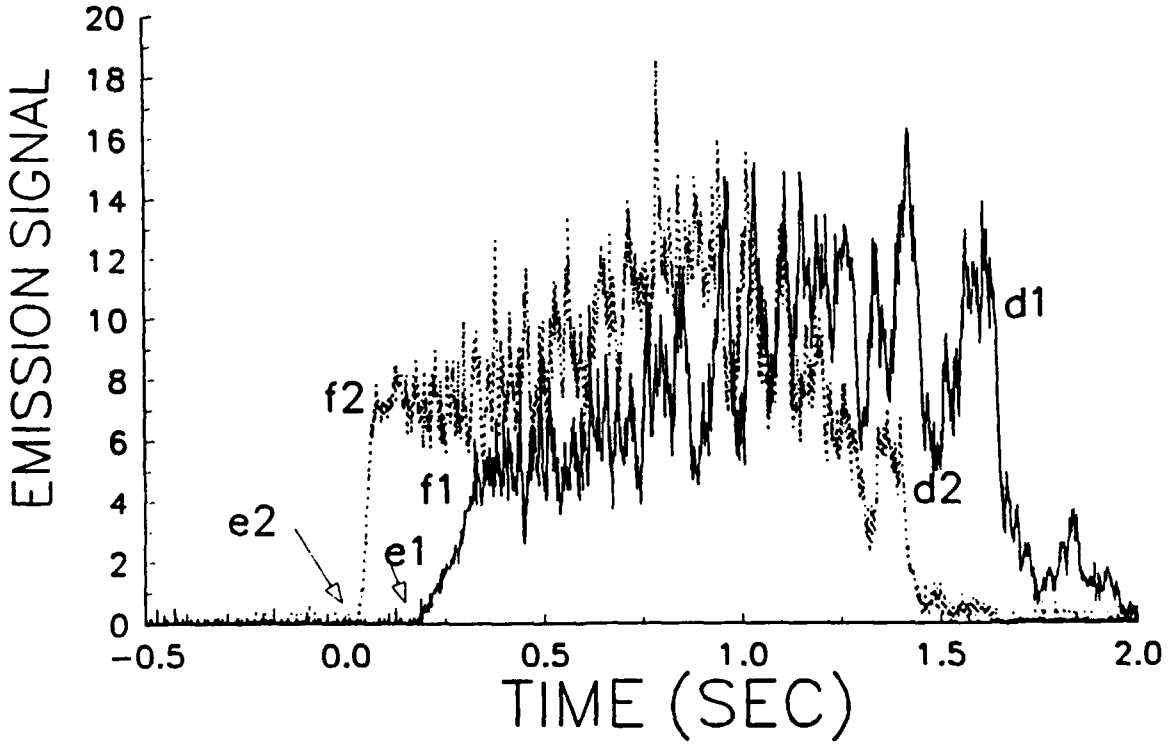

Figure 1. Photomultiplier records showing effect of flux level on emission from M9 in N_2.

The lines in Figure 2 are the ignition delays calculated from the model as a function of flux level for different heat release rates. "N" refers to a rate (given in Vilyunov and Zarko 1989) determined from radiant (black body) ignition experiments with the Russian double-base propellant N (0.58 NC, 0.28 NG, and 0.12 DNT), and "M9" refers to a rate determined from shock tube experiments with M9 (0.58 NC, 0.40 NG) powders in nitrogen (T = 600–700 K and pressure = 0.9–3.5 atm) (Cohen and Holmes 1982). For N and M9, Qz (cal/g-s) = 2.5E16 and 2.6E11, respectively. The corresponding values for E (kcal/mole) are 35 and 22. The rate for N propellant was determined from measurements of delays to observe a spike in the surface (thermocouple) temperature. The spike signaled the start of a rapid temperature increase presumably due to flamespreading. The rate for M9 was determined from emission delay measurements using small (<10 μm) particles uniformly heated (primarily) by conduction from reflected shock gas.

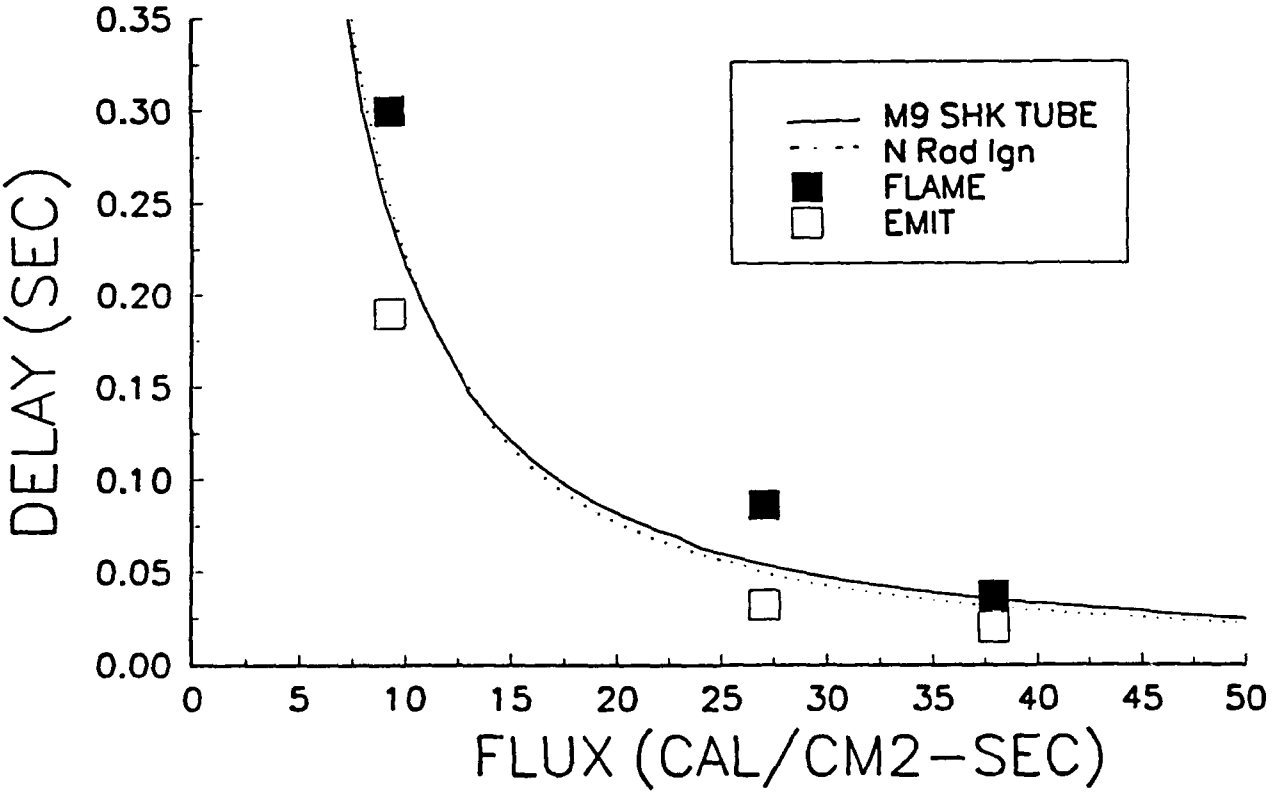

Figure 2. Comparison of emission and flamespreading delays for M9 in N_2 with calculations using heat release rates determined from radiative ignition and shock tube experiments.

At flux levels >10 cal/cm^2-s, (i.e., for calculated delays <0.3 s), differences between the calculated ignition delays are less than estimated measurement errors (flux ±10%, t_e ± 5%, and t_f ±15%).

The data are the t_e and t_f measurements with N_2 (in the bomb) initially at ambient conditions. Considering measurement errors and the uncertainties in thermophysical properties, both t_e and t_f appear to be in reasonable agreement with predictions of the "approximate" model.

Figures 3a, 3b, and 3c show the flux dependence of the t_{ig} calculation on the kinetic parameters Qz and E and the absorption coefficient n. The middle lines correspond to the one calculated for M9 in Figure 2a (Qz = 2.6E11, E = 22, and n = 536). The dependence on kinetic parameters decreases markedly at higher flux levels (>25 cal/cm^2-s). The dependence on n decreases markedly for absorption lengths (1/n) < 20 μ.

Figure 4 (and Table 1) show the effects of flux level and pulse duration on JA2 response to deradiation. The photomultiplier signals are from experiments in Ar at ambient conditions. The values of t_e and t_f decrease with increasing power, similar to the M9 results, but at higher power (and higher energy) and shorter pulse length, the final emission decay at d2 occurs at laser shutoff, t_l (i.e., deradiation leads to extinguishment). The only evidence of reaction in the recovered sample is a crater formed (primarily) in the irradiated region. Emission, in this case, is due to local gasification (laser-assisted combustion) reaction. At lower power and longer pulse lengths, reaction decelerates at t_l (corresponding to d1 in this figure), but recovers. Self-acceleration leads to the sharp increase in emission at f1 which is assumed to be the start of flamespreading. The subsequent decay (not shown) in emission is the result of propellant consumption.

The data in Figure 5 are the emission and "flamespreading" delays for JA2 in air and Ar at ambient conditions. The t_l values were used in place of the t_f values for air at 40 and for Ar at 4 cal/cm^2-s. These t_l values are approximately 10% less than the corresponding t_f measurements. The data at 90 cal/cm^2-s are from an experiment in room air. All others are from experiments in the bomb. The line is the calculated M9 ignition delay shown previously in Figure 2. The data near 40 cal/cm^2-s suggest that substitution of air for argon shortens t_f but does not affect t_e. The differences between calculation and measurements are probably within estimated measurement/thermophysical properties errors for t_e at the higher flux levels, but the differences are much greater for t_f.

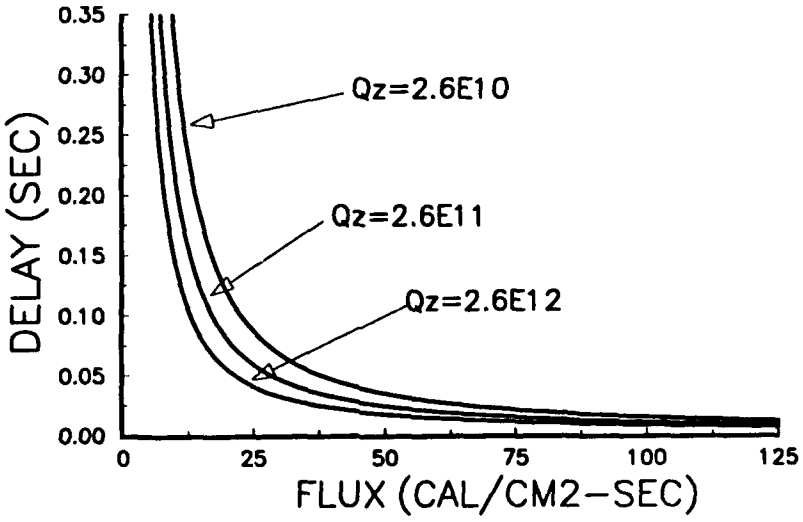

a. Kinetic pre-exponential Qz (cal/g-s).

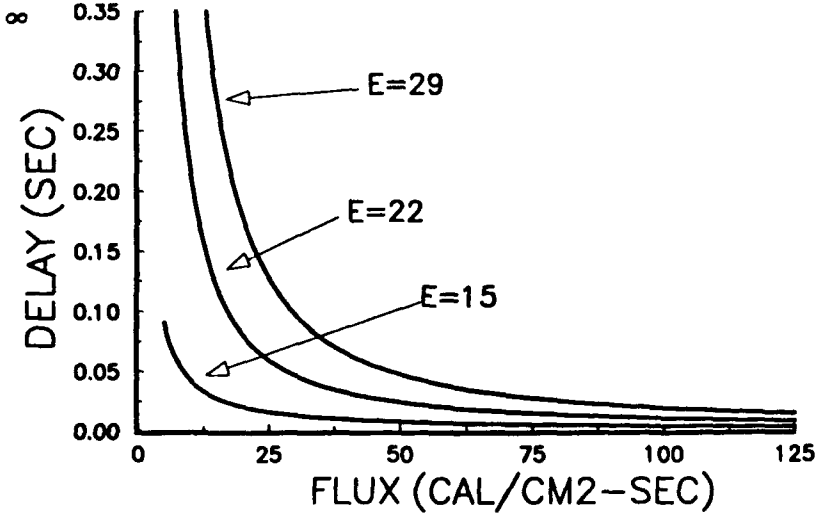

b. Kinetic activation energy E (kcal/mole).

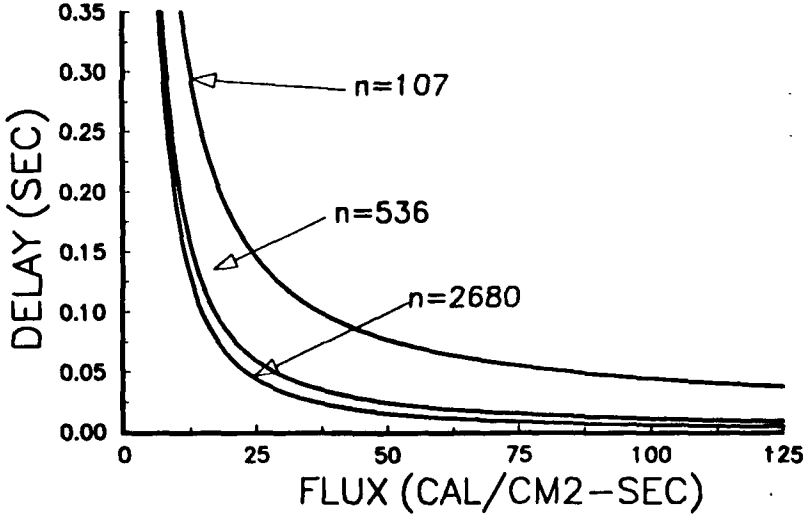

c. Absorption coefficient n (cm^{-1}).

Figure 3. Effect of input parameters on calculated ignition delays.

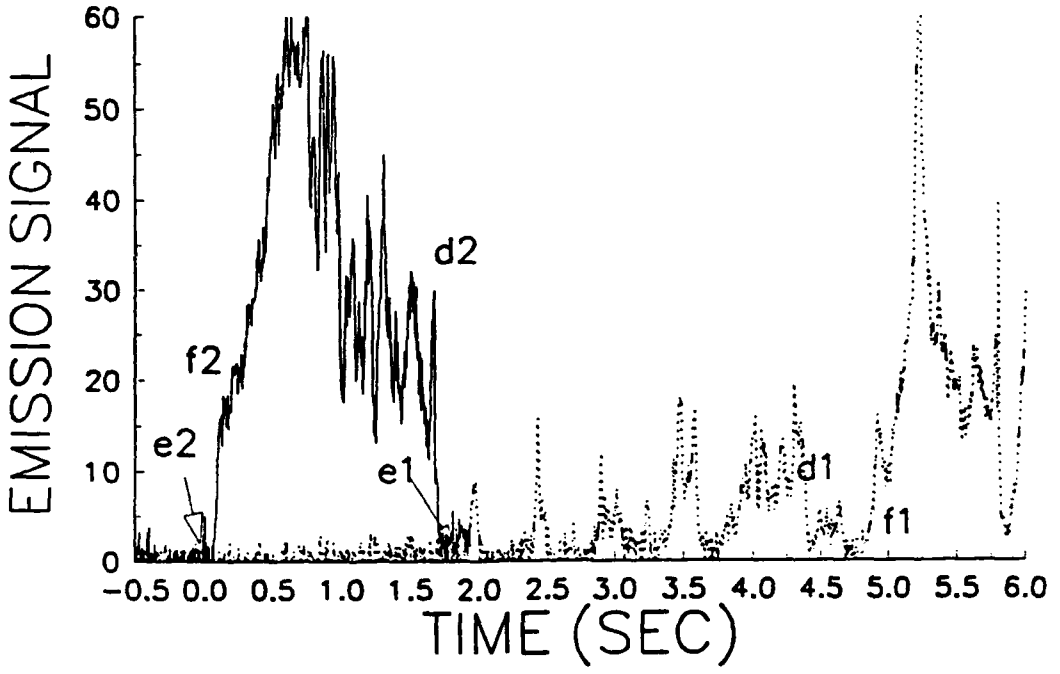

Figure 4. Photomultiplier records showing the effects of power and pulse length on reaction of JA2 in Ar.

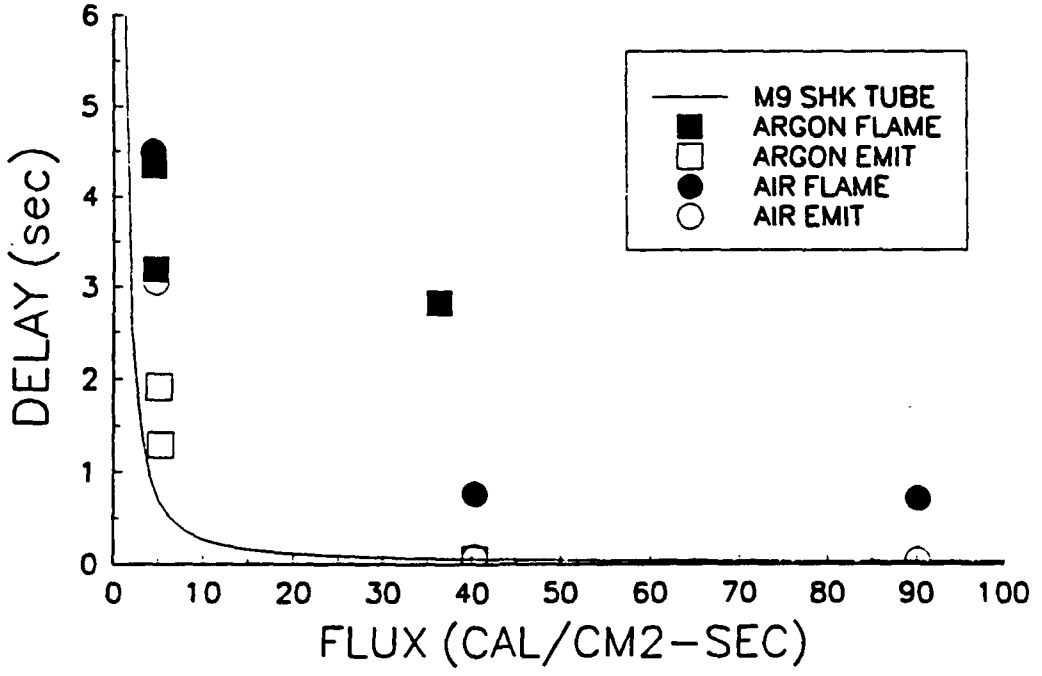

Figure 5. Comparison of emission and flamespreading delays for JA2 in Ar and air with calculations.

Figure 6 shows the emission signal during ignition of M30 in room air in which a transition from fizz (at f) to (visible) flame burning (at g) occurs. This transition has only been observed during irradiation (laser assisted) and differs from the transition to flamespreading with JA2, (at f1 in Figure 3) which occurs after deradiation. This suggests that absorption of laser radiation by M30 reaction products contributes to this transition.

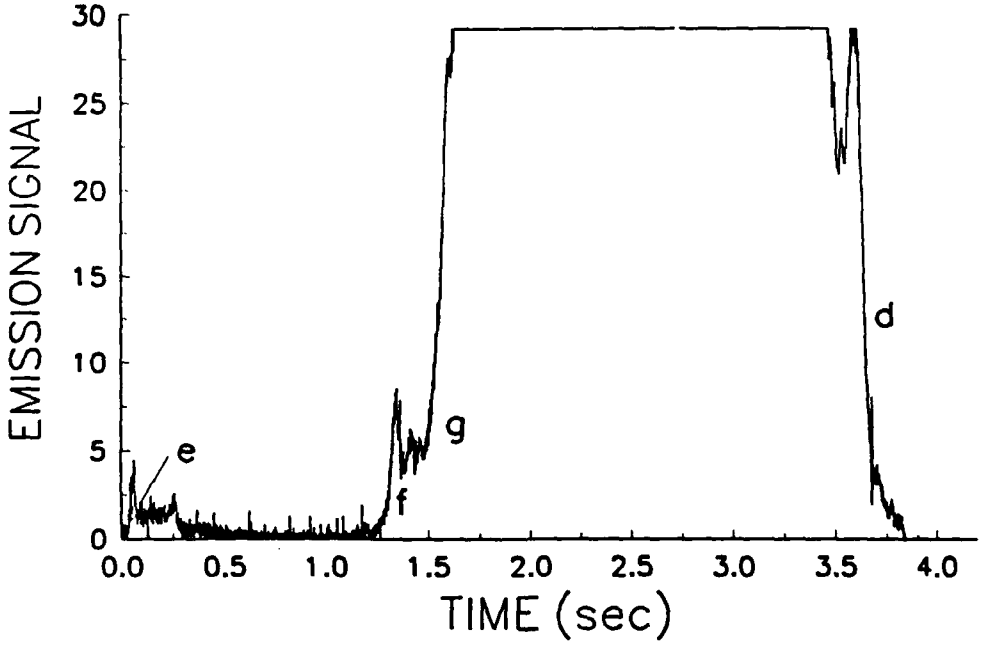

Figure 6. Photomultiplier records showing transition from fizz to flame burning for M30 in air.

The data in Figure 7 are the emission and "flamespreading" delays for M30 in room air and with N_2 in the bomb at ambient conditions. The line is the calculated M9 ignition delay. The results suggest that t_e values are not greatly different in air or N_2, and, except at low flux values, are in reasonable agreement with the M9 calculations. The t_f values (near 35 cal/cm^2-s) are less in air than in nitrogen and are much greater than calculations.

4.3.2 Nitramine Propellants. Figure 8 (and Table 1) show the effect of pulse length on the response of XM39 to deradiation. The emission signals are from experiments at fixed power in air initially at ambient conditions in the bomb. The initial spike in the emission signals may be due to RDX reaction. The difference in t_e values may reflect the stochastic nature of the ignition process. The initial propellant

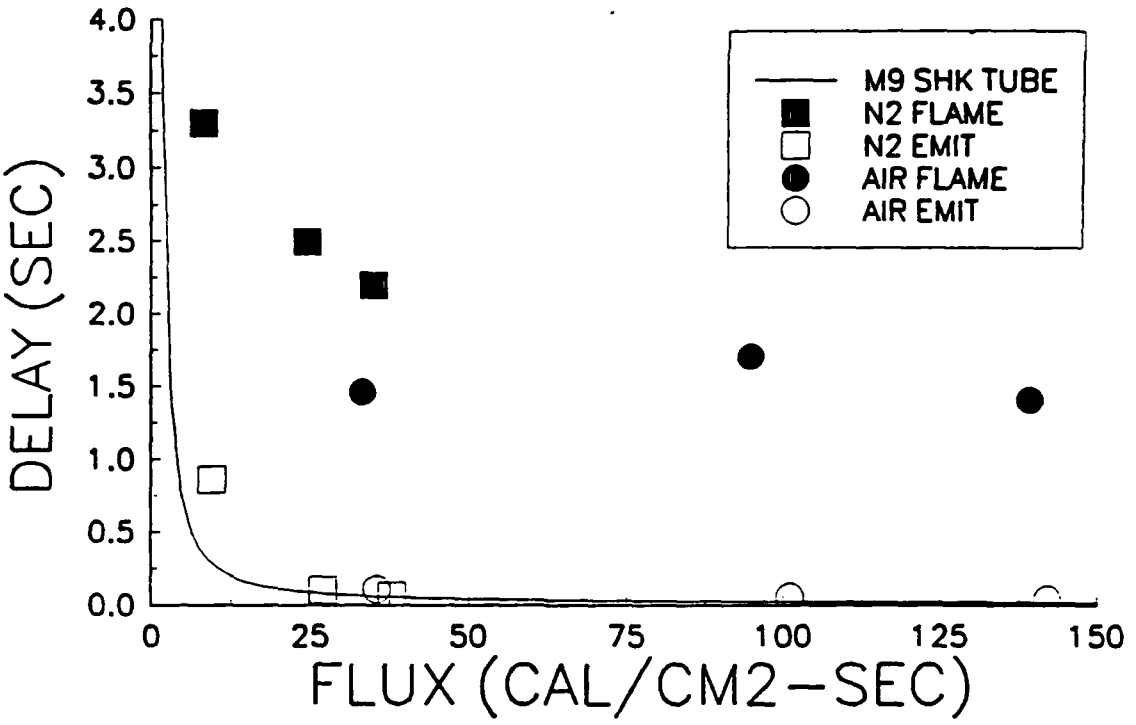

Figure 7. Comparison of emission and flamespreading delays for M30 in N_2 and air with calculations.

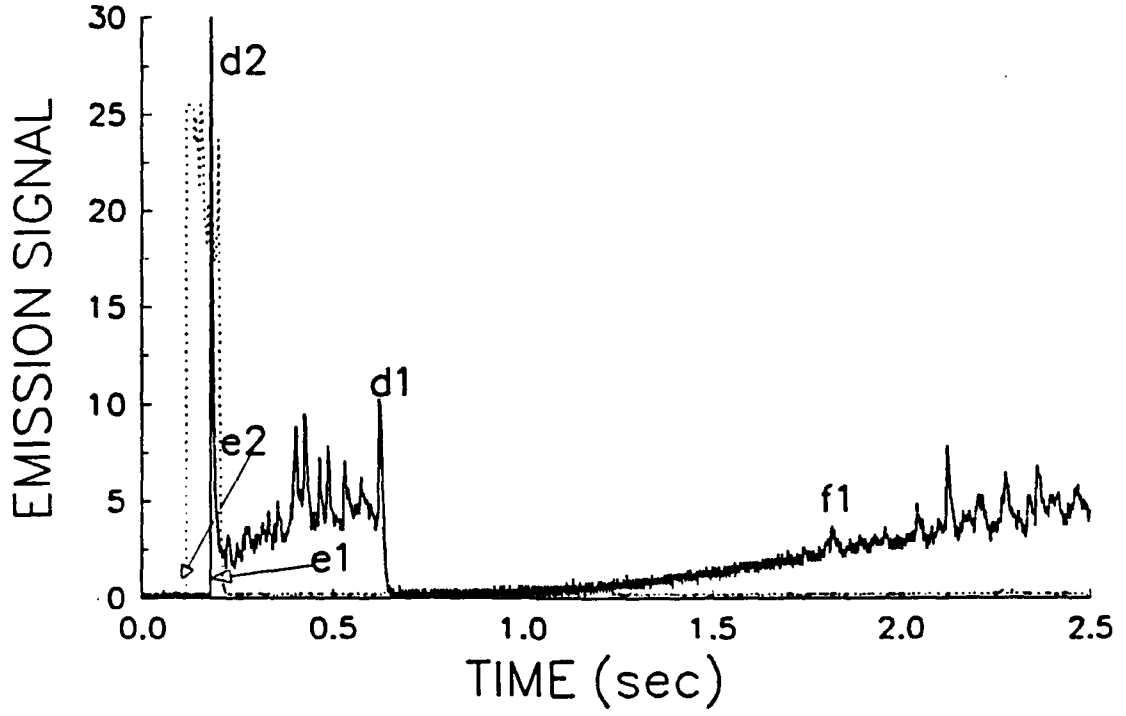

Figure 8. Photomultiplier records showing the effect of pulse length on reaction of XM39 in air.

response to deradiation is a sharp decay in emission. With the shorter pulse, reaction stops (at d2), leaving a crater at the irradiated surface. With the longer pulse, it recovers (at d1) and continues to self-accelerate. The final emission decay (not shown) is the result of propellant consumption.

The lines in Figure 9 are the calculated ignition delays as a function of flux levels using different heat release rates for XM39. "DSC" refers to a rate determined from DSC experiments with XM39 (Miller et al. 1988). In these experiments, the exothermic reaction was preceded by an endothermic reaction. For the calculations, the heat of the XM39 reaction was taken as the sum of both reactions and the heat release rate was taken as that of the exotherm. "Tcr" refers to a rate based on DSC experiments with RDX which was adjusted to give agreement between calculated and measured critical explosion temperatures for RDX (Rogers 1975). The rate for XM39 was obtained by multiplying the RDX rate by 0.75, which is approximately the mass fraction of RDX in XM39. The effect of the other constituents on the rate has been neglected for this calculation. The values of Qz(cal/g-s) for "DSC" and "Tcr" are 5.46E16 and 5.8E20, respectively. The corresponding values for E (kcal/mole) are 38.2 and 47.1. For flux levels >1 cal/cm^2-s, the differences between calculations are much less than measurement errors. The data are t_e values for XM39 with air and Ar, and t_l (pulse length) values (with air), all at ambient conditions in the bomb. Flamespreading was observed with air at flux levels >25 cal/cm^2, but not with Ar (i.e., infinite t_f). The t_l values were approximately 60% of the corresponding t_f values. The t_e values for air are in reasonable agreement with calculations, except at low flux levels. The t_f values are probably greater than calculated ignition delays. Comparison of the results with Ar and air indicates that O_2 accelerates the XM39 reactions responsible for both emission and flamespreading. DSC experiments are with inert atmospheres. This suggests that the DSC kinetics are not appropriate for XM39 (or RDX) reaction in air. The observed agreement between t_e for air and calculations may be fortuitous. It appears that the model and/or rates do not represent laser-initiated reaction in XM39 (for flux levels <47 cal/cm^2-s).

The lines in Figure 10 are the calculated ignition delays for HMX2 as a function of flux levels using different heat release rates. The line "SHK TUBE" refers to a rate for HMX2 determined from shock tube experiments with HMX powders in nitrogen (T = 690–740 K and approximate atmospheric pressure). "Tcr" refers to a rate based on DSC measurements with HMX, which have been adjusted to give agreement between calculated and measured critical explosion temperatures for HMX. The rates for HMX2 were obtained by multiplying the HMX rates by 0.8, which is the mass fraction of HMX in HMX2. The effect of the other constituents on the rate has been neglected for this calculation. The

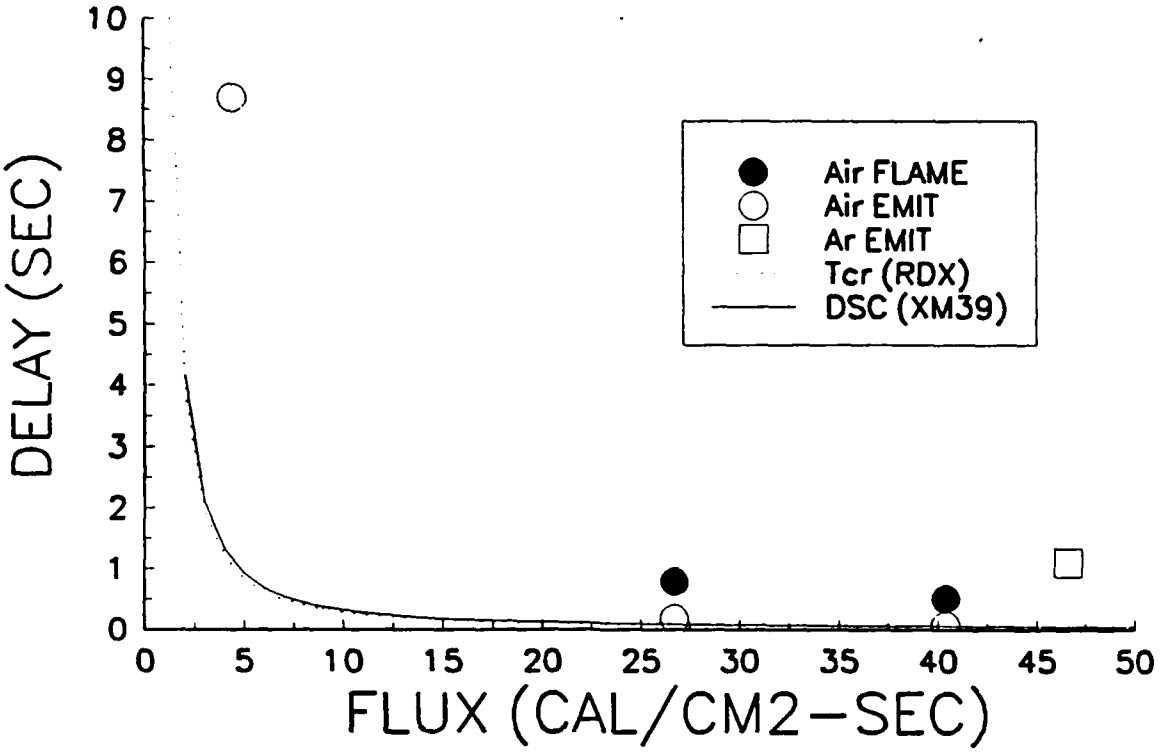

Figure 9. Comparison of emission and flamespreading delays for XM39 in Ar and air with calculations using heat release rates determined from DSC and critical temperature experiments.

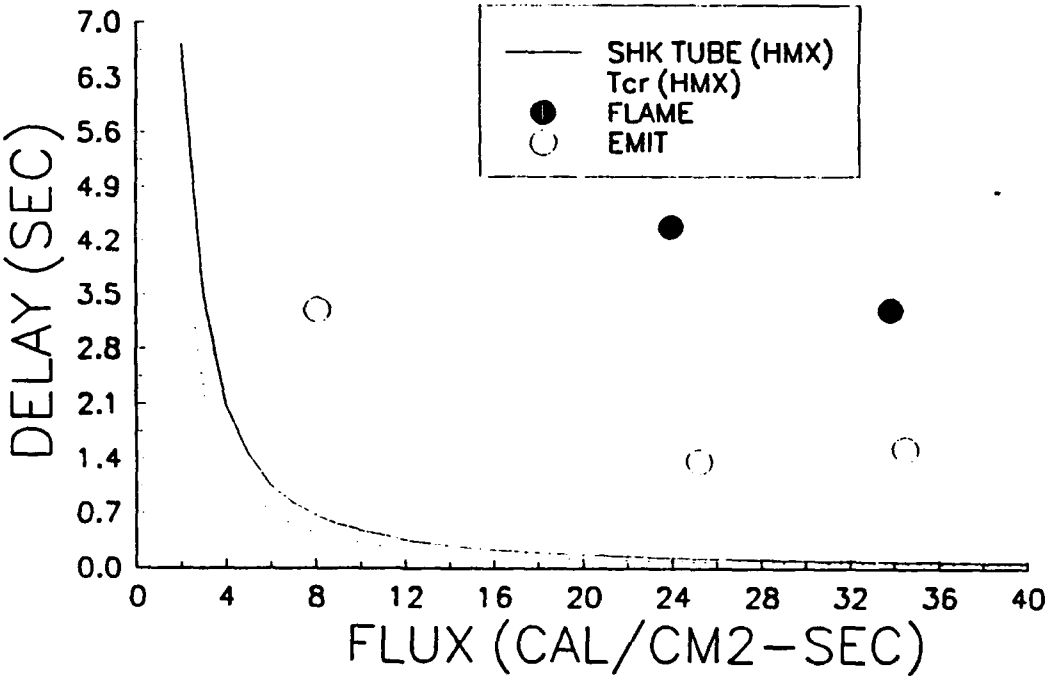

Figure 10. Comparison of emission and flamespreading delays for HMX2 in N_2 with calculations using heat release rates determined from shock tube and critical temperature experiments.

values of Qz (cal/g-s) for "SHK TUBE" and "Tcr" are 1.5E17 and 2.0E22, respectively. The corresponding values for E (kcal/mole) are 44.3 and 52.7. Calculated delays are noticeably shorter for the DSC rate at flux levels <20 cal/cm^2-s. The data are the emission and "flamespreading" delays for HMX2 in the bomb with nitrogen at ambient conditions. The values of t_e and t_f are much greater than the calculations, which indicates that the model and/or rates do not represent laser-initiated reaction in HMX2 (for flux levels <35 cal/cm^2-s).

5. COMMENTS

At this stage of the investigation, there is insufficient data to draw many firm conclusions concerning the modifications of the "approximate" model for use in the LIGHT program. The following are comments concerning requirements of a "useful" laser ignition model and some conclusions derived from the data.

1. The comparison of ignition model predictions and experimental delays implicitly assumes that the delays represent times required for the propellant reactions to generate conditions which satisfy the ignition criterion. For the "approximate" model, this requires that chemical reaction rates become large (infinite). At present, the validity of this assumption for either the measured emission delays or "flamespreading" delays is not known.

2. Although boundary conditions of model (1-D, uniform flux distribution) and experiment (2-D Gaussian flux distribution) differ, the model (and input parameters) appears to be able to predict M9 response to the CO_2 laser irradiation. It appears that both t_e and t_f are in reasonable agreement with model predictions, although, in principle, the ignition delay is unique. Which (if any) of the experimental delays corresponds to the calculated ignition delay and reasons for this dual agreement are, at present, not known. It also appears that at high flux levels and when using kinetics determined for M9, the model can reasonably predict the emission delays, but not the "flamespreading" delays of other nitrate ester propellants. However, the model does not appear to be appropriate for nitramine composite propellants.

3. The decrease in the flux dependence of the calculated ignition delay (for all kinetic rates) as flux levels increase suggests that precise knowledge of initiation rates will not be critical inputs into models of flamespreading at high flux levels.

4. The substitution of air for inert gases leaves t_e values for nitrate ester propellants unchanged, but shortens t_f values. This suggests that reaction of gases (O_2) affect flamespreading but not initiation.

5. The substitution of Ar for air with XM39 (nitramine) propellant appears to increase t_e and t_f values. This suggests that the reaction of gases (O_2) affect both initiation and flamespreading.

6. The laser-assisted transition from fizz to flame burning with M30 in air (Figure 6) suggests the possibility that laser absorption by reaction products aids in the transition. Knowledge of absorption coefficients and concentrations of these products will be required to predict this behavior.

7. Observations of deradiation and ambient gas effects similar to present observations but at higher pressures (5–20 atm) were reported in an early investigation of radiative ignition of double-base propellants (DeLuca et al. 1976a). The "approximate" model cannot be used to predict such effects.

These comments emphasize the shortcomings of the "approximate" model and imply that "useful" laser ignition models (for many propellants) need to include explicitly the effect of gas phase reactions on the physics of flamespreading.

INTENTIONALLY LEFT BLANK.

6. REFERENCES

Anderson, W. H. Combustion Science and Technology, vol. 5, pp. 75–81, 1972.

Cohen, A., and L. J. Decker. CPIA Publication 329, vol. 2, p. 469, 1980.

Cohen, A., and H. E. Holmes. "Convective Ignition of Double-Base Propellants." 19th Symposium (International) on Combustion, p. 691, The Combustion Institute, 1982.

DeLuca, L., T. J. Ohlemiller, L. H. Caveny, and M. Summerfield. "Radiative Ignition of Double-Base Propellants: I. Some Formulation Effects." AIAA Journal, vol. 14, no. 7, pp. 940–946, 1976a.

DeLuca, L., T. J. Ohlemiller, L. H. Caveny, and M. Summerfield. "Radiative Ignition of Double-Base Propellants: II. Pre-ignition Events and Source Effects." AIAA Journal, vol. 14, no. 8, pp. 1111–1117, 1976b.

Hermance, C. E. "Solid-Propellant Ignition Theories and Experiments." Fundamentals of Solid-Propellant Combustion, edited by K. K. Kuo and M. Summerfield, in Progress in Astronautics and Aeronautics, vol. 90, p. 239, 1984.

Kulkarni, A. K., M. Kumar, and K. K. Kuo. "Review of Solid Propellant Ignition Studies." AIAA Journal, vol. 20, no. 2, p. 243, February 1982.

Miller, M. S., A. J. Kotlar, A. Cohen, D. L. Puckett, H. E. Holmes, and K. Truong. "Effective Ignition Kinetics for LOVA Propellant." BRL-MR-3724, U.S. Army Ballistic Research Laboratory, Aberdeen Proving Ground, MD, December 1988.

Rogers, R. N. Thermochimica Acta, vol. 11, pp. 131–139, 1975.

Vilyunov, V. H., and V. E. Zarko. Ignition of Solids. Elsevier, Amsterdam, The Netherlands, 1989.

Williams, F. A. "Theory of Propellant Ignition by Heterogeneous Reaction." AIAA Journal, vol. 4, no. 8, August 1966.

INTENTIONALLY LEFT BLANK.

APPENDIX:

DERIVATION

INTENTIONALLY LEFT BLANK.

The derivation of the equations for calculating ignition delays from the "approximate" model (described in reference 4) are reproduced below (with typographical errors corrected).

The energy equations and the initial and boundary conditions for inert heating and adiabatic reaction are:

$$\frac{\partial T^I}{\partial t} = \alpha \frac{\partial^2 T^I}{\partial x^2} + \frac{q_o}{\rho c} n \exp(-nx)$$

$$T^I(x,0) = T_o \qquad T^I(\infty,0) = T_o \qquad \frac{\partial T^I}{\partial x}(0,t) = 0 \tag{1a}$$

$$\frac{dT^A}{dt} = \frac{QZ}{c} \exp\left(-\frac{E}{RT^A}\right) \qquad T^A(0) = T_1 \tag{1b}$$

where superscripts I and A refer to inert and adiabatic conditions, respectively. The corresponding nondimensional equations are obtained using the following:

$$\theta = \frac{1}{\beta}\left(\frac{T}{T_a} - 1\right), \quad \beta = \frac{RT_a}{E}, \quad \xi = \frac{x}{x_a}, \quad \tau = \frac{t}{t_a}, \quad \delta = \frac{q_o}{q_a}, \quad \mu = nx_a$$

$$x_a = \sqrt{\alpha t_a}, \quad q_a = \frac{\lambda \beta T_a}{x_a}, \quad t_a = \frac{\beta c T_a}{QZ} \exp(1/\beta), \quad \alpha = \frac{\lambda}{\rho c}$$

where the subscript a refers to standard values. The results are given by 2a and 2b

$$\frac{\partial \theta^I}{\partial \tau} = \frac{\partial^2 \theta^I}{\partial \xi^2} + \delta\mu \exp(-\mu\xi)$$

$$\theta^I(\xi,0) = \theta_o, \quad \theta^I(\infty,t) = \theta_o, \quad \frac{\partial \theta^I}{\partial \xi}(0,t) = 0 \tag{2a}$$

$$\frac{d\theta^A}{d\tau} = \exp\left(-\frac{\theta^A}{1+\beta\theta^A}\right) \qquad \theta^A(0) = \theta_1 \,. \tag{2b}$$

The inert solution is

$$\theta^I(\xi,\tau) = \theta_o + 2\delta\sqrt{\tau}\; i\phi^*(y) - \frac{\delta}{\mu}\exp(-\mu\xi) + \frac{\delta}{2\mu}\exp(-y^2)\left[\exp(w^2)\phi^*(w) + \exp(v^2)\phi^*(v)\right] \tag{3a}$$

where

$$y = \frac{\xi}{2\sqrt{\tau}}\,, \quad w = z - y\,, \quad v = z + y\,, \quad z = \mu\sqrt{\tau}$$

$$\phi^*(u) = 1 - \phi(u)\,, \quad \phi(u) = \frac{2}{\sqrt{\pi}}\int_o^u e^{-t^2}\,dt\,, \quad i\phi^*(u) = \frac{e^{-u^2}}{\sqrt{\pi}} - u\phi^*(u)\,.$$

The adiabatic solution is

$$\tau = \frac{1}{\beta^2 e^{1/\beta}}\left[F(x_1) - F(x)\right] \tag{3b}$$

where

$$x_k = \left\{\beta\left[1 + \beta\theta^A(\tau_k)\right]\right\}^{-1}\,, \quad F(u) = Ei(u) - \frac{\exp(u)}{u}$$

$$Ei(u) = \int_{-\infty}^{u}\frac{e^t}{t}\,dt$$

for $\xi = 0$

$$\theta^I(0,\tau) = \theta_o + \frac{2}{\sqrt{\pi}}\frac{\delta z}{\mu} + \frac{\delta}{\mu}\left[\exp(z^2)\,\phi^*(z) - 1\right] \tag{4a}$$

$$\frac{\partial \theta^I(0,\tau)}{\partial \xi} = \delta\mu \exp(z^2)\,\phi^*(z)\ . \tag{5a}$$

The inert heating time (t_h) and the corresponding surface temperature (T_h) are obtained from the "approximate" model assumptions, i.e., for $\xi = o$ and $\tau = \tau_h$, where $\tau_h = t_h/t_a$

$$\theta^I(0,\tau_h) = \theta^A(0) \tag{6a}$$

$$\frac{\partial \theta^I}{\partial \tau}(0,\tau_h) = \frac{d\theta^A(0)}{d\tau} \tag{7a}$$

let $T_a = T_h$

$$\theta^I(0,\tau_h) = 0 \tag{6b}$$

from (6a) $$\theta^A(0) = 0 \tag{6c}$$

from (2b) $$\frac{d\theta^A(0)}{d\tau} = 1 \tag{2c}$$

from (7a) $$\frac{\partial \theta^I(0,\tau_h)}{\partial \tau} = 1 \tag{7b}$$

from (4a) and (6b)

$$-\theta_o = |\theta_o| = \frac{2}{\sqrt{\pi}}\frac{\delta z_h}{\mu} + \frac{\delta}{\mu}\left[\exp(z_h^2)\,\phi^*(z_h) - 1\right] \quad \text{where} \quad z_h = \mu\sqrt{\tau_h} \tag{4b}$$

from (5a) and (7b) $$1 = \delta\mu \exp(z_h^2)\,\phi^*(z_h) \tag{5b}$$

$$\text{for } u >> 1 \qquad \exp(u^2)\,\phi^*(u) \simeq \frac{1}{\sqrt{\pi}\,u}\left(1 - \frac{1}{2u^2}\right) \tag{5c}$$

assume: $z_h >> 1$, $\mu^2|\theta_o| >> 1$

using (5c), (4b), and (5b)

$$2z_h^2 - \sqrt{\pi}\ z_h - \mu^2 \left|\theta_o\right| = 0 \tag{8}$$

solution of (8) gives

$$\tau_h \simeq \frac{\left|\theta_o\right|}{2} + \frac{1}{2\mu}\sqrt{\frac{\pi}{2}\left|\theta_o\right|}\ . \tag{9}$$

The equation used to solve for T_h is obtained from (9) and (5b):

$$\delta \simeq \frac{\pi}{4\mu} + \sqrt{\frac{\pi}{2}\left|\theta_o\right|}\ . \tag{10}$$

The dimensional form of (10) is quadratic in $\exp(E/RT_h)$. Real values for T_h are given by

$$\exp(E/RT_h) = \frac{\pi}{8}\,\frac{\lambda\rho QZ(T_h - T_o)}{q_o^2}\left[1 + \sqrt{1 + \frac{2q_o}{n\lambda(T_h - T_o)}}\right]^2. \tag{11}$$

T_h is obtained by numerical solution of (11).

t_a is calculated using $T_h = T_a$ and t_h is then obtained from (9).

The chemical induction time (t_{ch}) is obtained using the ignition criterion $\frac{d\theta}{d\tau} = \infty$ and (3b) in which is replaced by $\tau - \tau_h$:

τ

$$\tau - \tau_h = \frac{1}{\beta^2 \exp(1/\beta)}\left[F(x_1) - F(x)\right] \tag{3c}$$

where

$$x_k = \left\{\beta\left[1 + \beta\theta^A(\tau_k - \tau_h)\right]\right\}^{-1}$$

$$\text{for } u >> 1 \qquad Ei(u) \simeq \frac{\exp(u)}{u^2}\left(1 + \frac{1}{u} + \frac{2}{u^2}\right)$$

then

$$F(u) \simeq \frac{\exp(u)}{u^2}\left(1 + \frac{2}{u}\right)$$

assume

$$\beta << 1, \quad x >> 1, \quad x_1 >> 1$$

then (3c) can be written as

$$\tau - \tau_h \simeq (1 + 2\beta)\left[\frac{1}{\left(\frac{d\theta^A}{d\tau}\right)_{\tau_1}} - \frac{1}{\left(\frac{d\theta^A}{d\tau}\right)_{\tau}}\right] \tag{3d}$$

for $\tau_1 = \tau_h$ $\qquad \left(\frac{d\theta^A}{d\tau}\right)_{\tau_1} = 1$

for $\tau = \tau_{ig}$ $\qquad \left(\frac{d\theta^A}{d\tau}\right)_{\tau} = \infty$ $\qquad$ where $\tau_{ig} = \frac{t_{ig}}{t_a}$ and t_{ig} = ignition delay

from (3d) $\qquad \tau_{ch} = \tau_{ig} - \tau_h \simeq 1 + 2\beta$ $\qquad$ where $\tau_{ch} = \frac{t_{ch}}{t_a}$.

INTENTIONALLY LEFT BLANK.

No. of Copies	Organization
2	Administrator Defense Technical Info Center ATTN: DTIC-DDA Cameron Station Alexandria, VA 22304-6145
1	Commander U.S. Army Materiel Command ATTN: AMCAM 5001 Eisenhower Ave. Alexandria, VA 22333-0001
1	Director U.S. Army Research Laboratory ATTN: AMSRL-OP-CI-AD, Tech Publishing 2800 Powder Mill Rd. Adelphi, MD 20783-1145
1	Director U.S. Army Research Laboratory ATTN: AMSRL-OP-CI-AD, Records Management 2800 Powder Mill Rd. Adelphi, MD 20783-1145
2	Commander U.S. Army Armament Research, Development, and Engineering Center ATTN: SMCAR-IMI-I Picatinny Arsenal, NJ 07806-5000
2	Commander U.S. Army Armament Research, Development, and Engineering Center ATTN: SMCAR-TDC Picatinny Arsenal, NJ 07806-5000
1	Director Benet Weapons Laboratory U.S. Army Armament Research, Development, and Engineering Center ATTN: SMCAR-CCB-TL Watervliet, NY 12189-4050
1	Director U.S. Army Advanced Systems Research and Analysis Office (ATCOM) ATTN: AMSAT-R-NR, M/S 219-1 Ames Research Center Moffett Field, CA 94035-1000

No. of Copies	Organization
1	Commander U.S. Army Missile Command ATTN: AMSMI-RD-CS-R (DOC) Redstone Arsenal, AL 35898-5010
1	Commander U.S. Army Tank-Automotive Command ATTN: AMSTA-JSK (Armor Eng. Br.) Warren, MI 48397-5000
1	Director U.S. Army TRADOC Analysis Command ATTN: ATRC-WSR White Sands Missile Range, NM 88002-5502
(Class. only) 1	Commandant U.S. Army Infantry School ATTN: ATSH-CD (Security Mgr.) Fort Benning, GA 31905-5660
(Unclass. only) 1	Commandant U.S. Army Infantry School ATTN: ATSH-WCB-O Fort Benning, GA 31905-5000
1	WL/MNOI Eglin AFB, FL 32542-5000
	Aberdeen Proving Ground
2	Dir, USAMSAA ATTN: AMXSY-D AMXSY-MP, H. Cohen
1	Cdr, USATECOM ATTN: AMSTE-TC
1	Dir, ERDEC ATTN: SCBRD-RT
1	Cdr, CBDA ATTN: AMSCB-CII
1	Dir, USARL ATTN: AMSRL-SL-I
10	Dir, USARL ATTN: AMSRL-OP-CI-B (Tech Lib)

No. of Copies	Organization
1	HQDA, OASA (RDA) ATTN: Dr. C.H. Church Pentagon, Room 3E486 WASH DC 20310-0103
4	Commander US Army Research Office ATTN: R. Ghirardelli D. Mann R. Singleton R. Shaw P.O. Box 12211 Research Triangle Park, NC 27709-2211
2	Commander US Army Armament Research, Development, and Engineering Center ATTN: SMCAR-AEE-B, D.S. Downs SMCAR-AEE, J.A. Lannon Picatinny Arsenal, NJ 07806-5000
1	Commander US Army Armament Research, Development, and Engineering Center ATTN: SMCAR-AEE-BR, L. Harris Picatinny Arsenal, NJ 07806-5000
2	Commander US Army Missile Command ATTN: AMSMI-RD-PR-E, A.R. Maykut AMSMI-RD-PR-P, R. Betts Redstone Arsenal, AL 35898-5249
1	Office of Naval Research Department of the Navy ATTN: R.S. Miller, Code 432 800 N. Quincy Street Arlington, VA 22217
1	Commander Naval Air Systems Command ATTN: J. Ramnarace, AIR-54111C Washington, DC 20360
2	Commander Naval Surface Warfare Center ATTN: R. Bernecker, R-13 G.B. Wilmot, R-16 Silver Spring, MD 20903-5000

No. of Copies	Organization
5	Commander Naval Research Laboratory ATTN: M.C. Lin J. McDonald E. Oran J. Shnur R.J. Doyle, Code 6110 Washington, DC 20375
2	Commander Naval Weapons Center ATTN: T. Boggs, Code 388 T. Parr, Code 3895 China Lake, CA 93555-6001
1	Superintendent Naval Postgraduate School Dept. of Aeronautics ATTN: D.W. Netzer Monterey, CA 93940
3	AL/LSCF ATTN: R. Corley R. Geisler J. Levine Edwards AFB, CA 93523-5000
1	AFOSR ATTN: J.M. Tishkoff Bolling Air Force Base Washington, DC 20332
1	OSD/SDIO/IST ATTN: L. Caveny Pentagon Washington, DC 20301-7100
1	Commandant USAFAS ATTN: ATSF-TSM-CN Fort Sill, OK 73503-5600
1	F.J. Seiler USAF Academy, CO 80840-6528
1	University of Dayton Research Institute ATTN: D. Campbell AL/PAP Edwards AFB, CA 93523

No. of Copies	Organization
1	NASA Langley Research Center Langley Station ATTN: G.B. Northam/MS 168 Hampton, VA 23365
4	National Bureau of Standards ATTN: J. Hastie M. Jacox T. Kashiwagi H. Semerjian US Department of Commerce Washington, DC 20234
1	Applied Combustion Technology, Inc. ATTN: A.M. Varney P.O. Box 607885 Orlando, FL 32860
2	Applied Mechanics Reviews The American Society of Mechanical Engineers ATTN: R.E. White A.B. Wenzel 345 E. 47th Street New York, NY 10017
1	Atlantic Research Corp. ATTN: R.H.W. Waesche 7511 Wellington Road Gainesville, VA 22065
1	AVCO Everett Research Laboratory Division ATTN: D. Stickler 2385 Revere Beach Parkway Everett, MA 02149
1	Battelle ATTN: TACTEC Library, J. Huggins 505 King Avenue Columbus, OH 43201-2693
1	Cohen Professional Services ATTN: N.S. Cohen 141 Channing Street Redlands, CA 92373
1	Exxon Research & Eng. Co. ATTN: A. Dean Route 22E Annandale, NJ 08801

No. of Copies	Organization
1	General Applied Science Laboratories, Inc. 77 Raynor Avenue Ronkonkama, NY 11779-6649
1	General Electric Ordnance Systems ATTN: J. Mandzy 100 Plastics Avenue Pittsfield, MA 01203
1	General Motors Rsch Labs Physical Chemistry Department ATTN: T. Sloane Warren, MI 48090-9055
2	Hercules, Inc. Allegheny Ballistics Lab. ATTN: W.B. Walkup E.A. Yount P.O. Box 210 Rocket Center, WV 26726
1	Alliant Techsystems, Inc. Marine Systems Group ATTN: D.E. Broden/MS MN50-2000 600 2nd Street NE Hopkins, MN 55343
1	Alliant Techsystems, Inc. ATTN: R.E. Tompkins 7225 Northland Drive Brooklyn Park, MN 55428
1	IBM Corporation ATTN: A.C. Tam Research Division 5600 Cottle Road San Jose, CA 95193
1	IIT Research Institute ATTN: R.F. Remaly 10 West 35th Street Chicago, IL 60616
2	Director Lawrence Livermore National Laboratory ATTN: C. Westbrook M. Costantino P.O. Box 808 Livermore, CA 94550

No. of Copies	Organization
1	Lockheed Missiles & Space Co. ATTN: George Lo 3251 Hanover Street Dept. 52-35/B204/2 Palo Alto, CA 94304
1	Director Los Alamos National Lab ATTN: B. Nichols, T7, MS-B284 P.O. Box 1663 Los Alamos, NM 87545
1	National Science Foundation ATTN: A.B. Harvey Washington, DC 20550
1	Olin Ordnance ATTN: V. McDonald, Library P.O. Box 222 St. Marks, FL 32355-0222
1	Paul Gough Associates, Inc. ATTN: P.S. Gough 1048 South Street Portsmouth, NH 03801-5423
2	Princeton Combustion Research Laboratories, Inc. ATTN: N.A. Messina M. Summerfield Princeton Corporate Plaza Bldg. IV, Suite 119 11 Deerpark Drive Monmouth Junction, NJ 08852
1	Hughes Aircraft Company ATTN: T.E. Ward 8433 Fallbrook Avenue Canoga Park, CA 91303
1	Rockwell International Corp. Rocketdyne Division ATTN: J.E. Flanagan/HB02 6633 Canoga Avenue Canoga Park, CA 91304

No. of Copies	Organization
4	Director Sandia National Laboratories Division 8354 ATTN: R. Cattolica S. Johnston P. Mattern D. Stephenson Livermore, CA 94550
1	Science Applications, Inc. ATTN: R.B. Edelman 23146 Cumorah Crest Woodland Hills, CA 91364
3	SRI International ATTN: G. Smith D. Crosley D. Golden 333 Ravenswood Avenue Menlo Park, CA 94025
1	Stevens Institute of Tech. Davidson Laboratory ATTN: R. McAlevy, III Hoboken, NJ 07030
1	Sverdrup Technology, Inc. LERC Group ATTN: R.J. Locke, MS SVR-2 2001 Aerospace Parkway Brook Park, OH 44142
1	Sverdrup Technology, Inc. ATTN: J. Deur 2001 Aerospace Parkway Brook Park, OH 44142
1	Thiokol Corporation Elkton Division ATTN: S.F. Palopoli P.O. Box 241 Elkton, MD 21921
3	Thiokol Corporation Wasatch Division ATTN: S.J. Bennett P.O. Box 524 Brigham City, UT 84302
1	United Technologies Research Center ATTN: A.C. Eckbreth East Hartford, CT 06108

No. of Copies	Organization
1	United Technologies Corp. Chemical Systems Division ATTN: R.R. Miller P.O. Box 49028 San Jose, CA 95161-9028
1	Universal Propulsion Company ATTN: H.J. McSpadden 25401 North Central Avenue Phoenix, AZ 85027-7837
1	Veritay Technology, Inc. ATTN: E.B. Fisher 4845 Millersport Highway P.O. Box 305 East Amherst, NY 14051-0305
1	Brigham Young University Dept. of Chemical Engineering ATTN: M.W. Beckstead Provo, UT 84058
1	California Institute of Tech. Jet Propulsion Laboratory ATTN: L. Strand/MS 125-224 4800 Oak Grove Drive Pasadena, CA 91109
1	California Institute of Technology ATTN: F.E.C. Culick/MC 301-46 204 Karman Lab. Pasadena, CA 91125
1	University of California Los Alamos Scientific Lab. P.O. Box 1663, Mail Stop B216 Los Alamos, NM 87545
1	University of California, Berkeley Chemistry Deparment ATTN: C. Bradley Moore 211 Lewis Hall Berkeley, CA 94720
1	University of California, San Diego ATTN: F.A. Williams AMES, B010 La Jolla, CA 92093
2	University of California, Santa Barbara Quantum Institute ATTN: K. Schofield M. Steinberg Santa Barbara, CA 93106
1	University of Colorado at Boulder Engineering Center ATTN: J. Daily Campus Box 427 Boulder, CO 80309-0427
2	University of Southern California Dept. of Chemistry ATTN: S. Benson C. Wittig Los Angeles, CA 90007
1	Cornell University Department of Chemistry ATTN: T.A. Cool Baker Laboratory Ithaca, NY 14853
1	University of Delaware ATTN: T. Brill Chemistry Department Newark, DE 19711
1	University of Florida Dept. of Chemistry ATTN: J. Winefordner Gainesville, FL 32611
3	Georgia Institute of Technology School of Aerospace Engineering ATTN: E. Price W.C. Strahle B.T. Zinn Atlanta, GA 30332
1	University of Illinois Dept. of Mech. Eng. ATTN: H. Krier 144MEB, 1206 W. Green St. Urbana, IL 61801
1	The Johns Hopkins University Chemical Propulsion Information Agency ATTN: T.W. Christian 10630 Little Patuxent Parkway, Suite 202 Columbia, MD 21044-3200

No. of Copies	Organization
1	University of Michigan Gas Dynamics Lab Aerospace Engineering Bldg. ATTN: G.M. Faeth Ann Arbor, MI 48109-2140
1	University of Minnesota Dept. of Mechanical Engineering ATTN: E. Fletcher Minneapolis, MN 55455
3	Pennsylvania State University Applied Research Laboratory ATTN: K.K. Kuo H. Palmer M. Micci University Park, PA 16802
1	Pennsylvania State University Dept. of Mechanical Engineering ATTN: V. Yang University Park, PA 16802
1	Polytechnic Institute of NY Graduate Center ATTN: S. Lederman Route 110 Farmingdale, NY 11735
2	Princeton University Forrestal Campus Library ATTN: K. Brezinsky I. Glassman P.O. Box 710 Princeton, NJ 08540
1	Purdue University School of Aeronautics and Astronautics ATTN: J.R. Osborn Grissom Hall West Lafayette, IN 47906
1	Purdue University Department of Chemistry ATTN: E. Grant West Lafayette, IN 47906

No. of Copies	Organization
2	Purdue University School of Mechanical Engineering ATTN: N.M. Laurendeau S.N.B. Murthy TSPC Chaffee Hall West Lafayette, IN 47906
1	Rensselaer Polytechnic Inst. Dept. of Chemical Engineering ATTN: A. Fontijn Troy, NY 12181
1	Stanford University Dept. of Mechanical Engineering ATTN: R. Hanson Stanford, CA 94305
1	University of Texas Dept. of Chemistry ATTN: W. Gardiner Austin, TX 78712
1	Virginia Polytechnic Institute and State University ATTN: J.A. Schetz Blacksburg, VA 24061
1	Freedman Associates ATTN: E. Freedman 2411 Diana Road Baltimore, MD 21209-1525

USER EVALUATION SHEET/CHANGE OF ADDRESS

This Laboratory undertakes a continuing effort to improve the quality of the reports it publishes. Your comments/answers to the items/questions below will aid us in our efforts.

1. ARL Report Number ARL-TR-162 Date of Report July 1993

2. Date Report Received _____

3. Does this report satisfy a need? (Comment on purpose, related project, or other area of interest for which the report will be used.) _____

4. Specifically, how is the report being used? (Information source, design data, procedure, source of ideas, etc.) _____

5. Has the information in this report led to any quantitative savings as far as man-hours or dollars saved, operating costs avoided, or efficiencies achieved, etc? If so, please elaborate. _____

6. General Comments. What do you think should be changed to improve future reports? (Indicate changes to organization, technical content, format, etc.) _____

CURRENT ADDRESS

_____
Organization

_____
Name

_____
Street or P.O. Box No.

_____
City, State, Zip Code

7. If indicating a Change of Address or Address Correction, please provide the Current or Correct address above and the Old or Incorrect address below.

OLD ADDRESS

_____
Organization

_____
Name

_____
Street or P.O. Box No.

_____
City, State, Zip Code

(Remove this sheet, fold as indicated, tape closed, and mail.)
(DO NOT STAPLE)

DEPARTMENT OF THE ARMY

OFFICIAL BUSINESS

BUSINESS REPLY MAIL
FIRST CLASS PERMIT No 0001, APG, MD

Postage will be paid by addressee.

Director
U.S. Army Research Laboratory
ATTN: AMSRL-OP-CI-B (Tech Lib)
Aberdeen Proving Ground, MD 21005-5066

NO POSTAGE
NECESSARY
IF MAILED
IN THE
UNITED STATES